

Entanglement control via reservoir engineering in ultracold atomic gases

S. McENDOO¹, P. HAIKKA², G. DE CHIARA³, G. M. PALMA⁴ and S. MANISCALCO^{1,2}

¹ SUPA, EPS/Physics, Heriot-Watt University - Edinburgh, EH14 4AS, UK, EU

² Turku Center for Quantum Physics, Department of Physics and Astronomy, University of Turku FIN20014, Turku, Finland, EU

³ Centre for Theoretical Atomic, Molecular and Optical Physics, School of Mathematics and Physics, Queens University - Belfast BT7 1NN, UK, EU

⁴ NEST Istituto Nanoscienze-CNR and Dipartimento di Fisica e Chimica, Università degli Studi di Palermo via Archirafi 36, I-90123 Palermo, Italy, EU

received 29 November 2012; accepted in final form 28 February 2013

published online 2 April 2013

PACS 03.67.Bg – Entanglement production and manipulation

PACS 03.75.Gg – Entanglement and decoherence in Bose-Einstein condensates

PACS 67.85.Hj – Bose-Einstein condensates in optical potentials

Abstract – We study the entanglement of two impurity qubits immersed in a Bose-Einstein condensate (BEC) reservoir. This open quantum system model allows for interpolation between a common dephasing scenario and an independent dephasing scenario by modifying the wavelength of the superlattice superposed to the BEC, and how this influences the dynamical properties of the impurities. We demonstrate the existence of rich dynamics corresponding to different values of reservoir parameters, including phenomena such as entanglement trapping, revivals of entanglement, and entanglement generation. In the spirit of reservoir engineering, we present the optimal BEC parameters for entanglement generation and trapping, showing the key role of the ultracold-gas interactions.

Copyright © EPLA, 2013

Introduction. – Ultracold gases have recently emerged as an exciting playground for the simulation of complex many-body systems. The great level of control and cooling over neutral atoms in an optical lattice has opened new avenues for the study of quantum magnetism, disordered systems, long-range interactions, supersolidity, and the effect of non-Abelian fields, just to mention a few examples (see, for example, refs. [1,2]). A particularly rich area of research at the point between ultracold atoms, open quantum systems and quantum information is the study of quantum reservoir engineering.

Mesoscopic quantum systems can be viewed as a special form of environment: due to their low temperature and relatively small size, their quantum coherence leads to important effects. A Bose-Einstein condensate (BEC) is a typical example. Previous works have focused on the interaction of localised impurities immersed in a BEC [3]; others have studied the case of a lattice of impurities interacting with a BEC which leads to emission of phonons and dissipation for the impurities [4]. The collective dephasing of a two spatial states impurity was considered in [5], and the dynamics of a single impurity in a BEC

was recently investigated in [6–8]. Moreover, experiments realising the dynamics of a single impurity immersed in a BEC [9,10] have recently been reported. All these studies and experimental progress open the way to applications in quantum information processing that were, until recently, unrealistic.

In general, the presence of the ultracold gas surrounding the impurities gives rise to non-dissipative decoherence due to collisions between the BEC atoms and the impurity atoms. The literature on both entanglement decay and entanglement generation in the presence of dephasing environments has focused on certain paradigmatic models of environment with specific types of spectral densities [11–13]. In this paper we investigate for the first time a situation for which the entanglement dynamics can be modified by changing both the form of the spectrum and the distance between the impurities. Dissipative state preparation and entanglement generation have been theoretically proposed and experimentally realised in a number of physical contexts [14] in situations in which the environment induces a Markovian dynamics of the reduced system, governed by Lindblad master equations. In our

system a modification of the BEC scattering length is reflected in the form of the reservoir frequency spectrum, leading to a change in its Ohmicity character [6]. As a consequence we can investigate the optimal reservoir parameters to preserve entanglement, as well as the optimal conditions for entanglement generation from a separable state, in a system in which the open system dynamics cannot be described by Lindblad master equations. For completeness, we also consider discord as an example of a quantum correlation that exceeds those captured by entanglement [15]. This quantity describes correlations beyond those ascribable to classical physics and highlights the presence of quantum effects even in cases where there is no entanglement.

From a fundamental point of view our results pave the way to new experiments on basic aspects of open quantum systems. Indeed, they provide a physical example of an experimentally realisable bipartite open quantum system whose exact, and therefore non-Markovian, dynamics is described by a time-local master equation. This is important because, together with optical implementations [16], these systems could be used as testbeds for experimental verification of fundamental theorems of open quantum systems, thus giving an essential contribution to the thriving field of non-Markovian quantum dynamics [17]. More specifically, the two-impurities in BEC we discuss in this paper could be used to verify the simplest non-trivial generalisation of the Lindblad-Gorini-Kossakowski-Sudarshan (LGKS) theorem for commutative dynamical generators, as we briefly discuss in the second section.

The structure of the paper is the following. In the next section, we briefly recall the effective pure dephasing model and its dynamics for two qubits, and discuss its interest for fundamental tests of open quantum systems dynamics. In the following section we discuss the dynamics of both entanglement and quantum discord for different reservoir parameters. In the fourth section, we show the onset of entanglement generation and its dependence on the distance between the qubits and on the scattering length. Finally, we present our conclusions.

The model. – The system we consider consists of impurity atoms immersed in a Bose-Einstein condensate trapped in a shallow harmonic potential. In contrast to similar proposals in which the atoms were confined in an optical lattice in the Mott-insulator regime [3,4], in the present model we consider atoms trapped in a superlattice of wavelength λ , *i.e.*, in a linear array of deep double-well potentials [5]. We focus on two such impurities separated by distance D . The two minima of the double well are separated by a distance $L = \lambda/4$. Our qubit consists of the presence of one atom in the left or right well of the double well, denoted by $|0\rangle$ and $|1\rangle$, respectively. We assume a weakly interacting background gas treated using a Bogoliubov approach and neglect tunneling between the two wells.

In this model, the populations of the density matrix do not change with time, while the off-diagonal terms decay according to non-trivial time-dependent decoherence functions whose exact form was computed in [5]. For two qubits, the relevant decoherence functions are $\Gamma_0(t)$, $\Gamma_{\pm}(t) = 2\Gamma_0(t) \pm \delta(t)$, where

$$\Gamma_0(t) = \frac{2g_{AB}^2 n_0}{\pi^2} \int_0^\infty dk k^2 e^{-k^2 \sigma^2/2} \frac{\sin^2(E_k t/2\hbar)}{E_k(\epsilon_k + 2g_B n_0)} \times \coth\left(\frac{\beta E_k}{2}\right) \left(1 - \frac{\sin 2kL}{2kL}\right), \quad (1)$$

and

$$\delta(t) = \frac{2g_{AB}^2 n_0}{\pi^2} \int_0^\infty dk k^2 e^{-k^2 \sigma^2/2} \times \frac{\sin^2(E_k t/2\hbar)}{E_k(\epsilon_k + 2g_B n_0)} \coth\left(\frac{\beta E_k}{2}\right) \times \left(\frac{\sin 2k(D+L)}{2k(D+L)} + \frac{\sin 2k(D-L)}{2k(D-L)} - 2\frac{\sin 2kD}{2kD}\right). \quad (2)$$

Here, g_{AB} is the coupling between the impurity atoms and the condensate gas, g_B is the boson-boson coupling constant, n_0 is the condensate density, $\sigma = \sqrt{\hbar/m\omega}$, ω is the trapping frequency, E_k is the energy of the k -th Bogoliubov mode, $\epsilon_k = \hbar^2 k^2/2m_B$ and $\beta = 1/(\kappa_B T)$. When the qubits are infinitely far apart, they both decay with rate $\Gamma_0(t)$, but the closer they are the stronger is the influence of the common environment and the bigger is the cross talk term $\delta(t)$. Physically, the relevant decay rates in this case are $\Gamma_+(t)$ and $\Gamma_-(t)$, describing the dephasing of the super- and sub-decoherent two-qubit states, respectively [5]. For finite distance D , at short times each qubit decoheres independently while for larger times, determined by the ratio of the distance over the typical speed of sound, the effects of the common reservoir become apparent [5,6]. Increasing the distance between the two impurities allows for simulation of the dynamics of two qubits in local dephasing environments. Hence, by changing D , that is, the wavelength of the superlattice, one can pass from a common environment to an independent environment scenario.

For non-dissipative open quantum systems as the one we are studying, one can generalise the LGKS theorem and demonstrate that the dynamics is completely positive if and only if the decoherence factors Γ_0 , Γ_+ , and Γ_- are positive at all times. The physical implementation and verification of our model would allow then to verify the generalization of the LGKS theorem for the simplest non-trivial commutative open quantum system. Both the single-qubit dephasing case and the dephasing of two qubits in local environments, indeed, possess a random unitary representation and are therefore always completely positive.

Correlations for initially entangled states. – Let us consider the dynamics of entanglement between the

impurities, and its dependence on the system and reservoir externally controllable parameters. Due to their computational simplicity combined with their potential for entanglement and non-classical behaviour, we consider as initial states Werner states of the form

$$\rho_W^+ \equiv c|\Phi^+\rangle\langle\Phi^+| + \frac{1-c}{4}\mathbb{I}, \quad c \in [0, 1], \quad (3)$$

$$\rho_W^- \equiv c|\Psi^+\rangle\langle\Psi^+| + \frac{1-c}{4}\mathbb{I}, \quad c \in [0, 1], \quad (4)$$

where $|\Phi^+\rangle = (|00\rangle + |11\rangle)/\sqrt{2}$ and $|\Psi^+\rangle = (|01\rangle + |10\rangle)/\sqrt{2}$ are maximally entangled states. As an example, in the appendix, we discuss how to prepare the two qubits in the state given by eq. (3). As for the generation of the second class of initial states here considered, given by eq. (4), we note that all Bell states are equivalent up to local operations, *i.e.*, if we are able to create one then we can generate all others, therefore the procedure sketched in the appendix can be generalised accordingly. Werner states have applications in quantum information and quantum teleportation [18,19]. Additionally, they interpolate between maximally entangled and separable states, and therefore are ideal states for investigating entanglement dynamics in our system. For $c \leq 1/3$ the state is separable; above that, the state initially has non-zero concurrence which will time evolve as

$$C_W^\pm(t) = \max \left\{ 0, ce^{-\Gamma_\mp(t)} - \frac{1-c}{2} \right\}. \quad (5)$$

This formula shows that, if the system is initially prepared in a Werner state, the interaction with the condensates cannot increase the initial entanglement and in general leads to a loss of concurrence. However, as we will see in the following, by manipulating the system-reservoir parameters we can control entanglement dynamics and maximise the amount of stationary entanglement in the system. From eq. (5) we also see that, for an initial state of the form ρ_W^+ (ρ_W^-) the only decay rate which enters the dynamics is the collective decay rate $\Gamma_-(t)$ ($\Gamma_+(t)$).

It is worth noticing that, for the states here considered, $C_W^\pm(t)$ does not depend on the phase shifts $\Pi_{ij}(t)$. The behaviour of the concurrence depends primarily on three factors: the initial state parameter, c , the scattering length of the condensate, a_B , and the distance between the qubits, D . By varying these parameters, it is possible to obtain a wide range of entanglement dynamics for long times. Specifically, three different types of entanglement dynamics can be observed: i) sudden death of entanglement, ii) sudden death followed by revivals, iii) entanglement trapping.

Figure 1(a) shows the distribution of the types of entanglement behaviours for two qubits at a distance $D = 5\lambda$, where λ is the wavelength of the optical lattice, for varying initial parameters, c , and scattering lengths, a_B , measured in units of the natural ^{87}Rb scattering length a_{Rb} , for the initial state of eq. (3). The white region corresponds to entanglement sudden death, the medium blue region corresponds to sudden death followed by revivals and the dark

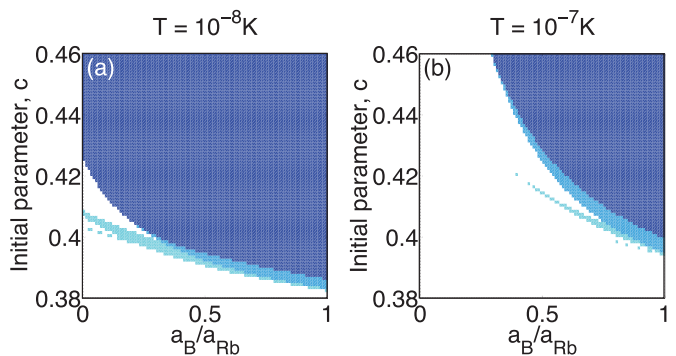


Fig. 1: (Colour on-line) Entanglement phase diagram for ρ_W^- as a function of scattering length, a_B in units of a_{Rb} , and initial state parameter, c , for $D = 5\lambda$ and (a) $T = 10^{-8}$ K and (b) $T = 10^{-7}$ K. We distinguish three phases: entanglement trapping (dark blue, top right), entanglement sudden death (white, bottom left) and entanglement revivals (medium blues) (see main text).

blue region corresponds to entanglement trapping. It is worth stressing the extreme sensitivity of the dynamics to the initial state, in the interval $0.38 \lesssim c \lesssim 0.46$. We recall that the state is separable for $c \leq 1/3 \simeq 0.33$. Entanglement sudden death takes place for small values of initial entanglement, that is, for $0.33 \lesssim c \lesssim 0.38$, while if the initial entanglement is sufficiently high the phenomenon of entanglement trapping, a non-zero value of stationary entanglement, will occur. This is the case for any value of $c \geq 0.425$, independently of the value of the scattering length, hence we can conclude that in this system entanglement trapping is dominant. In fact, for $c = 0.46$ the stationary entanglement is 0.19 for $D = 5\lambda$ at $T = 10^{-8}$ K. Under the same conditions a state with an initial concurrence $C_W^- = 1$ will retain a concurrence of $C_W^- = 0.8$. A similar entanglement phase-diagram exists for initial states of the form of eq. (4).

Entanglement trapping originates from the fact the time-dependent dephasing rates go to zero after a finite time. Hence dephasing stops and so does entanglement loss. This is a strongly non-Markovian phenomenon and never occurs for systems described by a master equation with positive constant decay rates.

In between the sudden death and entanglement trapping regions there are two small regions where entanglement exhibits periodic revivals which may or may not result in residual entanglement. It is worth noticing that, even when temperature is increased, there is still entanglement trapping for the majority of cases, as shown in fig. 1(b). The effect of the temperature is to enhance entanglement decay and enlarge the parameter space for which entanglement sudden death occurs. In fact, for typical experimental temperatures of the order of $T = 10^{-8}$ K to $T = 10^{-7}$ K entanglement trapping may only take place for sufficiently strongly interacting gases. In general, an increase in the scattering length of the ultracold reservoir will favour entanglement trapping, allowing for this phenomenon to occur for a wider class of initial states.

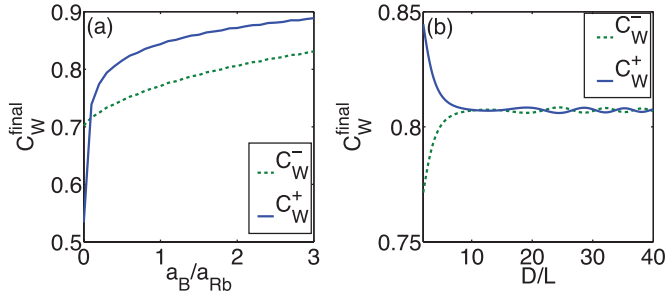


Fig. 2: (Colour on-line) (a) Stationary concurrence as a function of relative scattering length, a_B/a_{Rb} , for $D = \lambda/2$, $T = 10^{-8}$ K and for initial states ρ_W^- (green dashed line) and ρ_W^+ (blue solid line). (b) Steady-state value of concurrence, C_W^{final} , as a function of distance between qubits for initial states ρ_W^+ (blue solid) and ρ_W^- (green dashed) for $a_B = a_{Rb}$.

Moreover, as we can see from fig. 2(a), the stationary entanglement increases for increasing values of a_B , for both classes of initial states. This conclusion holds for any value of the distance D between the impurities. Hence we conclude that more strongly interacting gases are optimal for reaching higher values of entanglement trapping.

We now investigate the change in stationary entanglement when increasing the qubits separation, for a fixed value of the scattering length. Figure 2(b) shows C_W^- and C_W^+ as a function of D/L . Initially, there is an increase or decrease, respectively, of the entanglement, settling towards a steady value as the qubits get further apart. The different initial behaviour of stationary entanglement for the two classes of initial states can be explained as follows. When immersed in a common environment the initial states ρ_W^+ , which are mixtures of the subradiant state $|\Phi^+\rangle$, are sub-decoherent [5]. In our model an increase in the distances corresponds to a vanishing effect of the cross talk term, δ , and hence to a transition to a model of local dephasing for the impurities. For locally dephasing impurities sub-decoherence does not occur. This explains why an increase in the distance causes a decrease in the trapped entanglement for initially sub-decoherent states. The opposite holds for the other class of initial states ρ_W^- , which are super-decoherent in a common environment. In general, for large D , the cross talk term, δ , vanishes and the qubits behave as single qubits in independent reservoirs, eliminating the difference caused by their initial states. In terms of reservoir engineering, states ρ_W^+ are best protected from decoherence when immersed in a common environment, that is, for shorter values of the impurity separation due to smaller superlattice wavelength, while states ρ_W^- maximally retain the initial entanglement for longer impurity separations, that is, larger superlattice wavelengths.

We now look at the changes in the entanglement dynamics for different initial states and impurity distances. We focus our attention on the most interesting region of system-reservoir parameter space where the entanglement is most sensitive to the initial conditions. Figure 3(a) shows the concurrence for two qubits at $D = 2L = \lambda/2$,

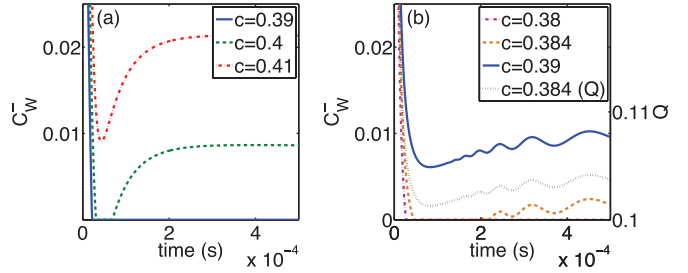


Fig. 3: (Colour on-line) Concurrence, C_W^+ , for (a) $D = \lambda/2$ for initial state parameters $c = 0.39$ (blue solid), 0.4 (green dashed) and 0.41 (red dotted), and (b) $D = 5\lambda$ for initial state parameters $c = 0.38$ (purple dotted), 0.384 (orange dashed) and 0.39 (blue solid). The grey dotted line represents the discord for $c = 0.384$.

that is, in adjacent pairs of sites of an optical lattice, for three values of the initial state parameter, c . As c increases, we can see the concurrence move from zero value to a finite value in the steady state. Figure 3(b) shows the same for qubits located at $D = 5\lambda$. At these distances the cross talk term, δ , picks up oscillations and the resulting concurrence shows more varied behaviour. In addition, the same initially entangled state will result in different concurrences for different values of D . In particular, for the same initial state, $c = 0.39$, the steady-state value of the concurrence changes from zero in fig. 3(a) to a small but non-zero value for fig. 3(b) due to the increased distance between qubits.

For the sake of completeness we conclude our analysis of correlations dynamics by looking at quantum discord of the impurities. In fig. 3(b) we compare discord and concurrence as a function of time for an exemplary initial state with $c = 0.384$. The concurrence shows an initial loss of entanglement, followed by periods of revival. The behaviour of the discord follows the same general trends as the concurrence, having peaks for the same instants of time. For this class of states, this is probably due to the simple dependance of both quantities on qubits correlations $\langle \sigma_z^A \sigma_z^B \rangle$ and $\langle \sigma_x^A \sigma_x^B \rangle$, where A and B denote the two qubits. An important difference, however, is that in the time intervals in which entanglement temporarily disappears, there are still oscillations present in the discord showing that the state still displays non-classical behaviours. This is not surprising as, in general, it is known that quantum discord is more robust against decoherence than entanglement and, for example, does not exhibit the phenomenon of entanglement sudden death.

Initial product states and entanglement generation. – One key advantage of a shared environment is its ability to generate correlations between initially separable states. In analogy to [13], we now consider how an initial product state,

$$|\psi(0)\rangle = \frac{1}{2} (|00\rangle + |01\rangle + |10\rangle + |11\rangle), \quad (6)$$

evolves in time. In contrast to Werner states in which only one of the decay rates, $\Gamma_{\pm}(t)$, would appear, for

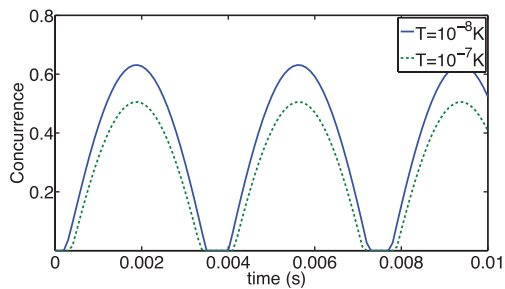


Fig. 4: (Colour on-line) Concurrence for the initial state of eq. (6) as a function of time for $T = 10^{-8}$ K (solid blue) and $T = 10^{-7}$ K (green dashed).

this initial state the dynamics is dictated by all three decay rates, including Γ_0 . Moreover in this case the entanglement crucially depends on the phase shifts $\Pi_{ij}(t)$. Figure 4 illustrates how the concurrence oscillates periodically between its zero value and a value close to its maximum 1, for temperatures of $T = 10^{-8}$ K. If the temperature is increased to $T = 10^{-7}$ K, the periodic generation of entanglement remains, but the maximum attainable concurrence is reduced. Eventually for $T > 10^{-6}$ K no concurrence is created. The limiting T can however be increased by increasing the qubit-BEC coupling.

The origin of this entanglement and the specific choice of the particular initial state (6) can be explained by the fact that the BEC induces an effective interaction Hamiltonian proportional to $\sigma_z^A \sigma_z^B$. This interaction creates conditional shifts between the two qubit impurities which, for a state of the form (6), correspond to an entangling operation. Therefore for other product states such as $|00\rangle$ or $|01\rangle$ we do not observe any entanglement generation at all.

We now explore how the generated entanglement can be maximised by varying reservoir parameters. Figure 5 shows the dependence of both the maximal entanglement and the generation time when one changes either the scattering length a_B or the distance D between the impurities. As the entanglement generation crucially relies on the phase factors, and as these quantities have negligible effect for increasing distances D , one sees that the maximum concurrence decreases with increasing distance while the generation time increases. On the other hand, the plots show that a more strongly interacting BEC leads to higher values of entanglement, that is, once more the optimal reservoir configuration is for higher values of a_B . The price to pay is a greater value of the generation time, indicating that one has to wait longer for the system to attain the highly entangled state.

Apart from fundamental implications for quantum reservoir engineering, our setup may have applications in optical lattices for the creation of long distance entanglement between impurities trapped in a superlattice. One does not need to manipulate the form of the impurities' potential by, for example, lowering and raising the barrier in a double well. One needs to control the time interval that impurities and BEC interact by moving

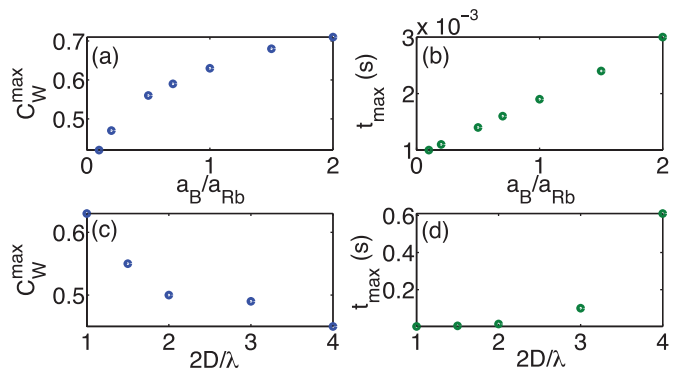


Fig. 5: (Colour on-line) (a) C_W^{max} , the maximum concurrence generated for the initial state of eq. (6), as a function of scattering length a_B/a_{Rb} for $D = \lambda/2$ and $T = 10^{-8}$ K. (b) t_{max} , the time at which the maximum concurrence of (a) occurs. (c) C_W^{max} , the maximum concurrence generated for the initial state of eq. (6), as a function of distance between qubits, D for $a_B = a_{Rb}$ and $T = 10^{-8}$ K. (d) t_{max} , the time at which the maximum concurrence of (c) occurs.

the impurities away from the BEC or by lowering to zero the interaction strength g_{AB} by means of Feshbach resonances.

Conclusions. – Atoms immersed in Bose-Einstein condensates provide an ideal system for investigating and probing many-body dynamics thanks to their interaction with the quantum excitations of the condensate. We have shown that double-well qubits in a Bose-Einstein condensate reservoir are a versatile system allowing controlled and robust entanglement generation and, at the same time, performing a quantum simulation of a paradigmatic non-Markovian open quantum system. For initially entangled Werner states, there is an initial loss of entanglement to the environment, but the presence of the common environment reduces, and in some cases partly reverses, the loss of correlations from the system to the environment. Moreover, for certain initially separable states, the BEC-induced effective interaction can generate entanglement between the two distant qubits. In the spirit of reservoir engineering, we have demonstrated how we can manipulate both the entanglement dynamics and the residual entanglement by modifying system reservoir parameters and we have shown that more strongly interacting BECs are optimal for both entanglement generation and entanglement trapping. If one aims at preservation of entanglement, then different classes of initial Werner states have opposite requirements ($D/L \simeq 1$ for ρ_W^+ and $D/L \gg 1$ for ρ_W^-), while entanglement generation is always optimal for small distances. Our study can be extended to multi-qubit systems in a straightforward way, by using the exact solution for n impurity qubits given in ref. [5].

Finally, we have shown that our results are robust to the effects of experimentally realistic temperatures, meaning that our proposal may be tested in present-day experimental setups. Our results pave the way to implementations of quantum communication protocols in arrays of quantum impurities and underline at the

same time the potential of these systems as testbeds for fundamental studies on open quantum systems in the non-Markovian regime.

This work was supported by EPSRC (EP/J016349/1), the Emil Aaltonen foundation, and the Finnish Cultural foundation. GMP acknowledges financial support from MIUR under project PRIN 2010-11 “Collective quantum phenomena: From strongly correlated systems to quantum simulators”. We acknowledge MARKUS CIRONE for useful discussions.

Appendix: experimental realisation. – The ideas and schemes presented in this work can be implemented using techniques realised in recent experiments of impurity-BEC dynamics. We consider an implementation with ^{133}Cs impurity atoms immersed in a ^{87}Rb condensate, but our results can be extended to other species or a single species BEC but with two different internal states. The impurities can be trapped by an optical superlattice with a double-well elementary cell, thus $D = 2L = \lambda/2$. For the case described in fig. 2(b) in which L and D are not in a simple ratio, one needs to use a different trapping mechanism for the impurities, for example arrays of microtraps [20] or of optical tweezers [21].

The initial Werner states considered in eq. (3) can be created using an entangling operation as the “square root of swap” $\sqrt{\text{SWAP}} = \exp[-i(\sigma_x^A \sigma_y^B - \sigma_y^A \sigma_x^B)\pi/8]$ operation realized in [22] as follows: i) prepare the two atoms in two distinct single wells; with probability c create the state $|10\rangle$ and with probability $1 - c$ create the maximally mixed state of the two qubits $\mathbb{I}/4$ by applying a fast random phase to an equal superposition of the two states $|0\rangle$ and $|1\rangle$ for the two atoms; ii) apply the $\sqrt{\text{SWAP}}$ gate by bringing the two atoms together, let them interact and separate them again; iii) finally transfer the internal state of each atom into the left and right states of the double well, that is, $|0\rangle \rightarrow |L\rangle$ and $|1\rangle \rightarrow |R\rangle$ using a spin-dependent potential and at the same time transforming each single well into a double well by raising the central barrier. To create the state $\rho_{\bar{W}}$ use $|01\rangle$ in stage i). A similar procedure, not involving the $\sqrt{\text{SWAP}}$ can be used to create state eq. (6).

Finally the readout can be achieved by transferring back the positional states $|L\rangle$ and $|R\rangle$ into the internal states $|0\rangle$ and $|1\rangle$ and then doing a full tomography of the two-qubit state. Fidelities of the order of 60% have been experimentally achieved [22], and these should be sufficient to demonstrate the generated entanglement. However for more accurate results methods based on the single-atom microscopy might be necessary [23].

REFERENCES

- [1] BLOCH I., DALIBARD J. and ZWERGER W., *Rev. Mod. Phys.*, **80** (2008) 885.
- [2] LEWENSTEIN M., SANPERA A. and AHUFINGER V., *Ultra-cold Atoms in Optical Lattices: Simulating Quantum Many-body Systems* (Oxford University Press, Oxford) 2012.
- [3] RECATI A., FEDICHEV P. O., ZWERGER W., VON DELFT J. and ZOLLER P., *Phys. Rev. Lett.*, **94** (2005) 040404; KLEIN A. and FLEISCHHAUER M., *Phys. Rev. A*, **71** (2005) 033605.
- [4] KLEIN A., BRUDERER M., CLARK S. R. and JAKSCH D., *New J. Phys.*, **9** (2007) 411.
- [5] CIRONE M. A., DE CHIARA G., PALMA G. M. and RECATI A., *New J. Phys.*, **11** (2009) 11 103055.
- [6] HAIKKA P., MCENDOO S., DE CHIARA G., PALMA G. M. and MANISCALCO S., *Phys. Rev. A*, **84** (2011) 031602.
- [7] MULANSKY F., MUMFORD J. and O’DELL D. H. J., *Phys. Rev. A*, **84** (2011) 063602.
- [8] PEOTTA S., ROSSINI D., POLINI M., MINARDI F. and FAZIO R., *Phys. Rev. Lett.*, **110** (2013) 015302.
- [9] WILL S., BEST T., BRAUN S., SCHNEIDER U. and BLOCH I., *Phys. Rev. Lett.*, **106** (2011) 115305.
- [10] SPETHMANN N., KINDERMANN F., JOHN S., WEBER C., MESCHEDE D. and WIDERA A., *Appl. Phys. B*, **106** (2012) 513519; SPETHMANN N., KINDERMANN F., JOHN S., WEBER C., MESCHEDE D. and WIDERA A., *Phys. Rev. Lett.*, **109** (2012) 235301.
- [11] PALMA G. M., SUOMINEN K.-A. and EKERT A. K., *Proc. R. Soc. London, Ser. A*, **452** (1996) 567.
- [12] WEISS U., *Quantum Dissipative Systems* (World Scientific) 1992.
- [13] BRAUN D., *Phys. Rev. Lett.*, **89** (2002) 277901.
- [14] DIEHL S. *et al.*, *Nat. Phys.*, **4** (2008) 878; WEIMER H. *et al.*, *Nat. Phys.*, **6** (2010) 382; BARREIRO J. T. *et al.*, *Nature*, **470** (2011) 486; KRAUTER H. *et al.*, *Phys. Rev. Lett.*, **107** (2011) 080503.
- [15] OLLIVIER H. and ZUREK W. H., *Phys. Rev. Lett.*, **88** (2001) 017901; HENDERSON L. and VEDRAL V., *J. Phys. A*, **34** (2001) 6899.
- [16] LIU B.-H., LI L., HUANG Y.-F., LI C.-F., GUO G.-C., LAINE E.-M., BREUER H.-P. and PILO J., *Nat. Phys.*, **7** (2011) 931.
- [17] See, for example: BREUER H.-P., LAINE E.-M. and PILO J., *Phys. Rev. Lett.*, **103** (2009) 210401; LAINE E.-M., PILO J. and BREUER H.-P., *Phys. Rev. A*, **81** (2010) 062115; RIVAS Á., HUELGA S. and PLENIO M., *Phys. Rev. Lett.*, **105** (2010) 050403; CHRUSCIŃSKI D., KOSSAKOWSKI A. and RIVAS Á., *Phys. Rev. A*, **83** (2011) 052128; LU X.-M., WANG X. and SUN C. P., *Phys. Rev. A*, **82** (2010) 042103.
- [18] HORODECKI M., HORODECKI P. and HORODECKI R., *Phys. Rev. A*, **60** (1999) 1888.
- [19] LEE J. and KIM M. S., *Phys. Rev. Lett.*, **84** (1999) 4236.
- [20] LENGWENUS A., KRUSE J., SCHLOSSER M., TICHELMANN S. and BIRKL G., *Phys. Rev. Lett.*, **105** (2010) 170502.
- [21] MULDOON C., BRANDT L., DONG J., STUART D., BRAINIS E., HIMSWORTH M. and KUHN A., arXiv:1109.0657 (2011).
- [22] ANDERLINI M., LEE P. J., BROWN B. L., SEBBY-STRAWLEY J., PHILLIPS W. D. and PORTO J. V., *Nature*, **448** (2007) 452.
- [23] WEITENBERG C. *et al.*, *Nature*, **471** (2011) 319; BAKR W. S. *et al.*, *Science*, **329** (2010) 547.